Design choices and thermal simulations of a new test cell facility

G. Cattarin[1,*], F. Causone[1], A. Kindinis[2], L. Pagliano[1]

[1] end-use Efficiency Research Group, Department of Energy, Politecnico di Milano, Via Lambruschini 4, 20156, Milano, Italy

[2] Université Paris-Est, Institut de Recherche en Constructibilité, ESTP, F-94230, Cachan, France

*Corresponding author: giulio.cattarin@polimi.it

Abstract

The paper presents a new test cell facility, named Box Office and under development at the Ecole Spéciale des Travaux Publics (ESTP Paris) for the analysis and characterization of the thermo-physical properties of building envelope components under real climate conditions.

The facility will allow to obtain reliable estimates of thermal performance indicators of transparent and opaque building elements. Particular care has been taken in the design phase in order to minimize or to monitor all sources of uncertainty, such as (i) conductive heat losses through the test cell envelope, (ii) time lag of response to transient outdoor conditions, (iii) levels of airtightness and of resistance to vapour or water penetration.

Highly variable solar conditions can seriously affect both the correct functioning of outdoor test facilities and the indoor climate conditions in the cell. For this reason, the thermal behaviour of the Box Office was simulated in Matlab environment, implementing a lumped-parameter model, and results are used for refining the design choices and selecting the most promising operative conditions and control strategies.

The output of test cell experiments will be beneficial to various target groups, such as designers and manufacturers (to boost the research and development of new products), research centres (to fully understand and model the physical phenomena occurring in a controlled space facing real outdoor conditions) and potential clients, who ask for economically affordable solutions guaranteeing high levels of Indoor Environmental Quality.

Keywords: *test cell, building envelope, experimental test, outdoor facility, guarded hot box*

1. Introduction

A broad variety of complex building envelope components have entered the building construction market during the last decades [1]. These elements are often characterized by a dynamic response to the outdoor climate and by features which can be adapted to the local climate, to the building use and to the desired architectural aesthetics. Many of these components have been claimed to present high thermal performance while improving occupants' comfort conditions. In this scenario, it is of crucial importance to test and characterize correctly these elements under real dynamic weather conditions, in order to analyse their behaviour and evaluate their effectiveness in improving building performance, by means of existing or ad-hoc performance indicators. Both indoor laboratory and outdoor test cells can be used for the purpose, presenting peculiar differences that make them complementary facilities. The present paper highlights the main features of the test cell under construction at the Ecole Spéciale des Travaux Publics, du Bâtiment et de l'Industrie (ESTP Paris) within the framework of a collaboration between the end-use Efficiency Research Group of Politecnico di Milano and ESTP.

Figure 1: a 3D perspective of the new test cell facility under development at ESTP (Paris)

2. The concept of the Box Office facility

A detailed physical analysis and design activity has been performed by the research team in order to minimize or to accurately evaluate all sources of uncertainty, The design choices have been based on a wide literature review, on interviews to experts in IEA ECBCS Annex 58 (Reliable Building Energy Performance Characterisation Based on Full Scale Dynamic Measurements) and DYNASTEE network and on an intense information exchange with constructors of calorimeters and suppliers of data acquisition systems.

The first issue to address has concerned the control of heat flows through the test cell envelope. Various design approaches have been proposed so far, including:

- Local measurement of heat exchanges: test cells can be provided with a grid of large-area heat-flow meters applied to the internal surfaces of the walls; they enable to measure the heat flows passing through the envelope. This solution has been extensively developed within PASLINK project [2], and has been recently upgraded for the test cell built in Florence and described by Alcamo [3].

- Other test cells - such as the EMPA outdoor facility described by Manz et al. [4] - are surrounded by a thermally-controlled (guard) zone. The air temperature difference between the metering zone and the guard zone must be kept as small as possible in order to minimize heat exchanges between those two zones.

The decision of adopting a guard zone for the test cell at ESTP has been based on the following considerations:

- Guard zones allow to minimize heat losses down to values that cannot be obtained by means of thick insulation layers. This is of particular interest in tests for determining the thermal transmission (U-value) of building components.

- The first method (grid of large-area heat flow meters) presents some potentially critical issues, such as (i) the necessity to periodically calibrate a large number of sensors (ii) the additional complexity introduced by the high number of sensors used (PASLINK test cells use about 240 Heat Flux Sensitive Tiles), which entails the risks of sensors' malfunctioning/failures and a greater amount of data needed to calculate the heat balance of the test cell.

Looking at the traditional guarded test cell, with internal dimensions of the metering zone (usually called test room) typical of a real office space (e.g. LxWxH = 5m x 3m x 3m) at least three potential problems can be detected:

- The test room presents a high thermal inertia: this has a negative effect on the responsiveness of the system during transient conditions.

- The test room presents a large surface area of envelope compared to the surface area of the test sample. In case of a non-optimal control over the guard zone, the heat losses through the test room envelope can become non-negligible with respect to the heat losses through the test element;

- It may be difficult to reach a full mixing in the guard zone, and this can result in a non-uniform surface temperature distribution on the external side of the metering zone envelope. Even when the thermostat in the guard zone detects a temperature equal to that of the test room, there may be actually local heat fluxes crossing the two zones, due to local temperature differences into the guarded zone;

The choice of the internal dimensions of the test room is justifiable just in view of having an indoor space that is representative of a real office, but it is not optimal for a calorimetric approach.

In order to address these issues, the first step in the design process of the Box Office facility has been the decoupling of Indoor Environmental Quality (IEQ) tests from calorimetric tests.

This has led to a configuration by which the calorimetric tests are carried out in a dedicated metering box, while the IEQ tests are carried out in a room. A scheme of both configurations for the operation of the test cell is presented in Figure 2.

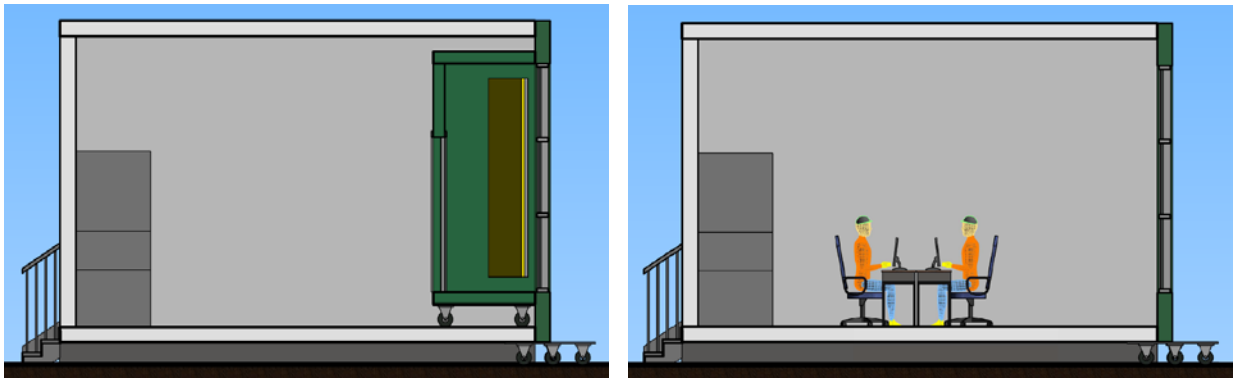

Figure 2. On the left: configuration used for the calorimetric tests: the test sample is applied on the aperture of the metering box, while the guard zone closely follows the air temperature in the box. On the right: configuration adopted for Indoor Environmental Quality tests, having removed the metering box.

Compared to the traditional guarded test cell, the suggested solution presents the following advantages:

1) Response time. The small volume of air and the small surface area (and mass) of the box walls allow to rapidly control the internal temperature of the box in order to keep the set-point. In addition, a solar absorber has been designed for the purpose of removing the entering solar gains (visible in *Figure 2*). As already mentioned, the response time of the metering zone is a very important feature when the aim is analysing the solar factor at varying solar incidence angles.

2) Heat loss minimized. Unwanted heat losses are reduced because the surface ratio between test component (3m x 3m) and the rest of the envelope of the metering zone passes from 20% to 40% (as the depth of the metering zone passes from 500 to 120 cm). The reduction of surface area causes a reduction of potential conductive heat losses (the reduction is less than linearly proportional, since thermal bridges become proportionally more influent).

3) Temperature uniformity on the external sides of the metering box. The air in the guard zone can be easily well-mixed, reducing the risk of surface temperature non-uniformity on the external side of the metering box;

4) Airtightness. The small dimensions of the metering box and the possibility to move the box on wheels when fixing it to the test component give additional guarantees on the airtightness of the system. A tracer gas test before each experimental campaign will determine the airtightness level achieved.

In addition, the possibility to remove the metering box allows to perform tests on thermal and visual comfort

and (under certain configurations) ventilation effectiveness in the guard zone. The guard zone internal dimensions are representative of an office room and it offers a good control over environmental conditions (temperature stability will be in a range of ±0,5 °C). A photoacoustic gas analyser can be used to perform tests on contaminant distribution. This type of test can be conducted, for example, when characterizing prefabricated elements including a decentralized ventilation system. The guard zone will be equipped with air and surface temperature sensors according to the methodology proposed by PASLINK [5] and COMPASS projects [6]. In this case, the guard zone will not be used following a calorimetric approach.

3. Modelling the Box Office

The design of a test cell is a delicate phase, and a hasty decision influences the facility performance for its whole operational life. For this reason, the thermal behaviour of the Box Office is being simulated in Matlab environment, and results are used for refining the design choices.
In particular, the test cell is represented by a lumped-parameter model. Lumped models are closely correlated to physical characteristics of the thermal system and they allow for an intuitive graphical representation in the form of resistive-capacitive (RC) circuits. The main hypotheses underpinning lumped models can be found in [7], while examples of studies applying lumped models to buildings are given in [8]-[10].
More information on the features of the test cell, and in particular on the cooling system constituted by the solar absorber mentioned in the previous section, will be provided while describing the model hypotheses.

3.1 Envelope of the metering zone and test component

According to the design, the envelope of the metering zone (the box) will be constructed with prefabricated sandwich panels, formed by two 0.6 mm stainless steel sheets and 15 cm thick injected-polyurethane foam insulation (see Table 1). The resulting thermal conductance is equal to 0.153 W m^2 K^{-1}.
The whole envelope of the metering zone is treated as a single third-order element (4R3C). There is no need to assign a node to each wall, since they all present the same stratigraphy and are exposed to environments with homogeneous air temperatures (i.e. the metering zone and the guard zone). In addition, it is not necessary to consider separately a ground node (e.g. as done in [11] and [12]) because the box is lifted from the floor of the guard zone by means of a metallic wheeled structure (see Figure 1 and Figure 2, left).

Material	Thickness [mm]	Thermal conductivity [$Wm^{-1}K^{-1}$]	Specific heat capacity [$Jkg^{-1}K^{-1}$]	Density [kg m^{-3}]
steel sheet	0.6	50.0	500	7800
polyurethane foam	150.0	0.023	1500	40
steel sheet	0.6	50.0	500	7800

Table 1: Stratigraphy of the metering zone envelope.

The test component considered is a double-glazing façade of dimensions 3 m x 3 m, with a transparent area equal to 9 m^2. This means that the test sample covers the whole available aperture of the metering box. The test sample has a global thermal transmittance U = 2.1 W m^{-2} K^{-1}, a solar direct transmittance τ_{test} = 0.7 and a thermal absorption coefficient α_{test} = 0.17. As a first approximation, τ_{test} and α_{test} are considered constant properties, independent from the solar incidence angle. This assumption can be considered valid when running the simulation for a limited time lapse (e.g. 1 hour), during which the solar incidence angle presents limited variations. Usually, the nominal τ_{test} reported in technical specifications corresponds to a perpendicular incident radiation, and represents the maximum value among all possible incidence conditions. Here it is considered constant to analyse the most critical condition in terms of entering solar gains.

The overall heat transfer coefficient (UA value) of the test component takes into account eventual thermal bridges, corner effects and any other imperfection e.g. due to the installation phase. The thermal capacitance of the test sample is estimated around $3.42*10^5$ J K^{-1}, thus it cannot be neglected since it represents about 17 % of the overall thermal capacity of the system (including the box envelope, the solar absorber filled with

water and the internal air). When more massive thermal systems are investigated (such as residential or tertiary buildings), the thermal capacitance of transparent elements may be neglected, thus treating glazing components as purely resistive elements (see e.g. [11]-[13]).

A graphical representation of this portion of the overall model is provided in *Figure 3*. The average temperatures of the absorber plate (T_{met}) and the insulation layer on the rear of the absorber (T_{ins}) are coloured to indicate that they are dynamically determined during the simulation, as discussed in the next section.

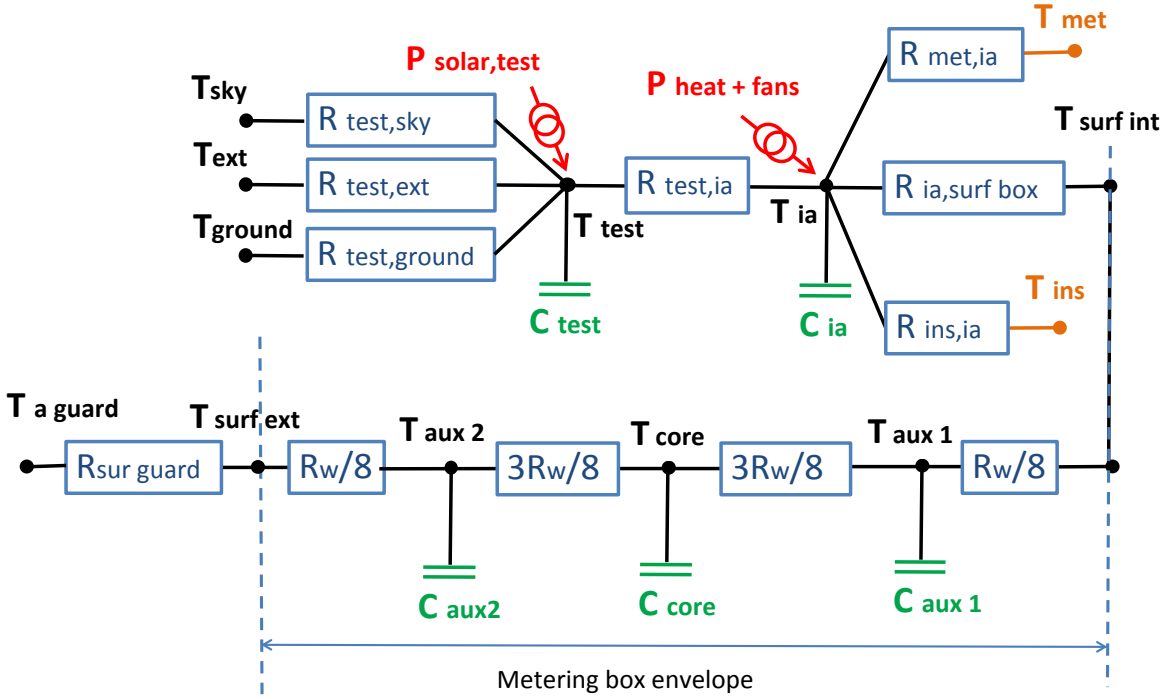

Figure 3. RC representation of the thermal model under study (to be coupled to the RC model of the solar absorber).

The focus of the present simulations is the thermal behaviour of the metering zone, which is the actual control volume for calorimetric tests. The guard zone is thus considered as an ideal space kept at same set-point temperature of the metering zone. Preliminary simulations show that sinusoidal variations of the air temperature in the guard zone with a period of 30 min and amplitude of 2 °C have a negligible effect on the dynamics of the Box envelope, thus is it reasonable to simplify the description of the guard zone considering it an “ideal space” at constant $T_{set\text{-}point}$.

3.2 The solar absorber

The solar absorber is a heat exchanger in charge of the removal of the entering solar gains. It acts as a two-parallel plate solar thermal panel, though, in the present case, the useful effect is the cooling of the box and not the heating of the circulating fluid. Although the function is different, several similarities between the two technological solutions make it reasonable to model the solar absorber on the basis of the experience gained on solar thermal panels (see e.g. [14]-[17]).

Discretized models that subdivide the solar collector along the fluid direction are considered to better reproduce temperature spatial distribution and get better results on the outlet fluid temperature [17].
In the present case, in order to investigate the correct number of water nodes to consider in the model, preliminary simulations have been conducted, focusing the attention on the water temperature at the outlet of the solar absorber. The results have shown that 5 nodes are largely sufficient to describe the temperature profile along the direction of the flow, while keeping the overall model simple enough for fast calculations.
The solar absorber is thus discretised in the vertical direction (floor to ceiling) into 5 elements of width 3.0 m and height 0.5 m, and assumed as perfectly flat. Following the hypotheses originally adopted by Kamminga [15] and Schnieders [16] for a flat-plate solar collector, edge effects as well as horizontal temperature

gradients are considered negligible and the only temperature gradients taken into account are i) in the direction of the water flow and ii) across the different layers of the absorber. The assumption of a uniform temperature in the horizontal direction actually implies two underlying assumption: an equal distribution of the circulating fluid in the channels and a uniform distribution of solar radiation on the absorber plate. Finally, conduction phenomena within the water and between adjacent elements of the metal plate are neglected. The present model dynamically provides the temperatures of three layers:

- the average temperature of the absorber plate $T_{met,j}$

- the average temperature of circulating fluid (distilled water) $T_{w,j}$

- the average temperature $T_{ins,j}$ of the insulation layer on the plate back

Assigning an average temperature to the insulation layer may seem a rough approximation, since its temperature profile presents a strong gradient between the average temperature of the circulating water and that of the internal air. However, the simplification is reasonable when the aim is only considering the additional thermal capacity (C_{ins}) playing a role in the dynamics of the solar absorber.
Figure 4 illustrates the thermal network model of the solar absorber, with the three-layered elements represented in a different line style.

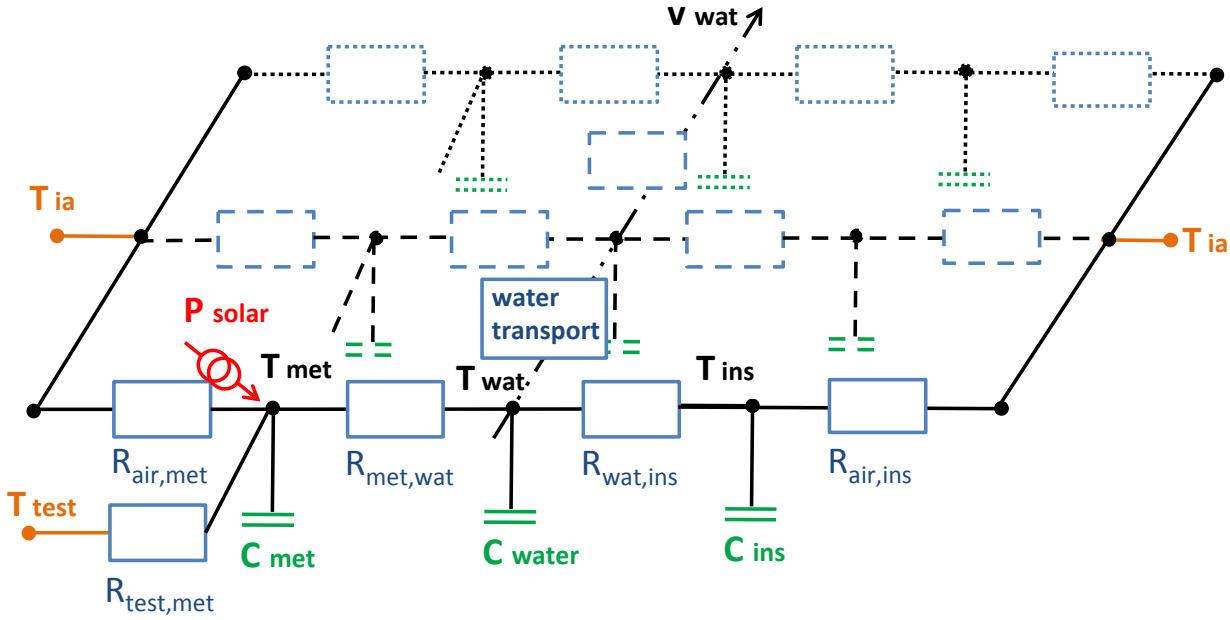

Figure 4. Thermal network model of the solar absorber. For ease of reading, the radiative heat exchange between the solar absorber and the test panel is represented only for the node on the foreground. The arrow v_{wat} indicates the direction of the fluid flow.

A final consideration is that, in a traditional solar collector exposed to outdoor air, part of the absorbed energy is lost to the ambient by convection with the external air and long wave radiation with the surroundings (mostly sky). This means that the collector efficiency decreases as the difference between the mean temperature of the collector and the ambient temperature increases. In the present case, the solar absorber is positioned inside the box, where the air is kept at a certain set-point (e.g. 26°C), and its average temperature is lower than the one of the internal air and the inner surface of the test sample. As a consequence, the absorber plate will remove heat respectively by convection and long-wave radiation, in addition to the cooling effect due to the removal of impinging solar radiation. Compared to the outdoor solar collectors, in the present case, the long-wave radiative and convective heat exchanges are not inefficiencies, since they contribute to the useful effect which is the removal of entering solar gains.

3.3 Weather conditions

The test cell facility will be installed in the campus of the ESTP Paris, located in the suburban area of Cachan. As concerns the weather conditions, the Test Reference Year of the weather station of Paris

Montsouris (about 3.5 km far) has been analyzed, in order to identify the most critical boundary conditions in terms of global solar irradiance. The data were processed by mean of the building energy simulation software TRNSYS in order to evaluate the maximum global solar irradiance impinging on a vertical surface exposed to south (here Gv), and the maximum temperatures of external air, sky and ground surface in the sunniest days. The most critical conditions over the whole TRY occur in October, when Gv $\approx$ 900 W m^{-2}. The external air and ground temperature are fixed at 20°C, while the sky temperature is fixed at 16°C.

High and rapidly-varying levels of solar irradiance are, as previously highlighted, the most critical conditions when the aim is guaranteeing the respect of a fixed set-point temperature. For this reason, several scenarios have been considered:

- steady solar irradiance at 900 W m^{-2}
- linear increase of the solar irradiance from 700 to 900 W m^{-2} in a time span of 10 min (simulating a rapid variation due to the passage of a transient cloud)
- sinusoidal variation of solar irradiance with period 15 min and amplitude 100 W m^{-2} varying around a mean value of 900 W m^{-2}

Previous measurements taken at the local weather station of ESTP have shown that the global solar irradiance does not vary more than 100 W m^{-2} on a time lapse of 5 min.
No shadowing effects have been considered, since they depend on the surroundings and on the geometry of the test sample under study (e.g. overhangs and window reveals). In the specific case, the Box Office facility will be positioned with its south façade facing an open meadow, thus the hypothesis of unobstructed exposition is well met, and it can thus be assumed that the test sample exchanges equally with the ground and the sky. A ground reflectance of 0.25, typical of short grass lawns, has been chosen for the calculation of reflected solar irradiance.

3.4 Other hypotheses

The heating system consists of four 250 W electrical resistances that can be modulated by means of a solid-state relay. Radiative heat exchanges due to the electric heater are minimized by placing the heater in an insulated box, thus treating its input heating power as purely convective.
The heating power is adjusted by a PI controller, which is fed by an error signal defined as: $\varepsilon = T_{set\text{-}point} - T_{ia}$. The controller is initially tuned on the basis of Ziegler–Nichols rules [18] for closed loops and then adjusted according to the simulation results.

Recirculation fans operate continuously in order to keep the internal air well-stirred and enhance the convective heat exchanges with the surface of the solar absorber. Thanks to their operation, the internal air can be assumed at uniform temperature and represented by a single node with its thermal capacitance. The fans constitute the main contribution to internal gains (estimated at 250 W).

The heat balance on internal air does not include terms of air renovation, since the system works in complete recirculation and is assumed to be perfectly airtight. The assumption of perfect airtightness also implies that the internal air does not experience any variation of absolute humidity, and thus no moisture balance equation is considered. Prior to the experiments, the internal air will be dehumidified to minimize condensation phenomena on the cold surface of the solar absorber, a phenomenon that would introduce uncertainties on a short-term heat balance.
Last but not least, important hypotheses concern the radiative and convective heat transfer coefficients to be adopted within the simulations. In particular, the water velocity in the solar absorber and the air velocity in proximity of the surfaces of the test sample and the solar absorber have a great influence on the thermal performance of the metering box, and are operational parameters that can be adjusted for control purposes, acting on the water pump and the recirculation fans.
A detailed description of the convective and radiative phenomena goes beyond the purpose of the present paper, and it will be addressed in a future publication.
Both models are integrated using the ODE15i solver provided by Matlab and based on an implicit scheme, characterized by unconditional stability, and, for the present case, a reasonable computational time (the solver requires about 8 sec for a 2-hours simulation).

The initial conditions have a significant impact in the short-term behaviour of a system [18]. For this reason, a "dummy simulation period" is simulated: the model is initially run for 120 min adopting the initial conditions reported in Table 1 until the system has settled, and then additional 60 min are simulated. Table 1 presents the initial conditions adopted for the dummy period. The temperatures of the air inside the metering zone (T_{ia}) and the guard zone (T_{guard}) are set to the set-point value, and the same applies to the temperatures inside the metering-box envelope (T_{aux1}, T_{core}, T_{aux2}). The heating power is initially off, while the recirculation fans are running. The water mass-flow rate is set at 0.40 kg s^{-1}, resulting in a water velocity of 0.027 m s^{-1}.

Table 1. Initial conditions

	value	**unit**
$T_{set-point}$	26	°C
T_{ia} , T_{guard} , T_{aux1}, T_{aux2}, T_{core}	$T_{set-point}$	°C
T_{inlet}	7	°C
water mass flow rate	0.40	kg s^{-1}
P_{heat}	0	W

4. First simulation results and discussion

At present (June 2015), the first thermal simulations are providing useful information on the key factors to consider for: i) the sizing of the heating and cooling system (e.g. maximum power levels, dimensions of the solar absorber), ii) the control of the operational parameters (e.g. inlet temperature and mass flow rate in the solar absorber, air velocity in the cavity between the test sample and the absorber plate, risks of rapid and undesired fluctuations of the electrical power input etc.).

Figure 5 presents the results obtained with a solar irradiance varying sinusoidally between 700 and 900 Wm^{-2}. The top figure shows the temperature profiles of the box envelope. In particular, it can be noticed that:

- the temperatures inside the metering box envelope (T_{aux1}, T_{core}, T_{aux2}) are stable at the set-point temperature of 26.0°C;
- the cooling power (calculated as $P_{cool}=Q_m*c_p*\Delta T$, where Q_m is the water mass flow rate, c_p the specific heat capacity of water and ΔT the temperature difference between inlet and outlet of the solar absorber) varies in a range between 5000 W and 5700 W, the higher values corresponding to the peaks of solar irradiance (with a slight time shift, due to thermal inertia effects;
- the outlet water temperature varies in a range between 10.0 °C and 10.4°C;
- the heating power varies between 60 and 120 W, and is frequently adjusted (the maximum adjustment frequency was set to 30 seconds);
- the test sample reaches an average temperature of about 32.6°C, while the temperature of the absorber plate varies between 17.8 °C and 19.6 °C

The results suggest the following considerations:

- the wall surfaces of the metering box are solicited only by small temperature variations of the internal air around the set-point, while radiative phenomena have been excluded considering that the solar absorber shades the internal zone. Since the temperatures of the internal nodes aux1, core and aux2 keep stable, it seems reasonable to assume that no heat is flowing to or form the guard zone. This simplifies heat balance calculations, since the box envelope can be considered adiabatic;
- the solar absorber provides the necessary cooling power even under critical solar irradiance conditions (Gv=900 W m^{-2});
- the outlet water temperature is about 3 °C higher than the inlet temperature. It is important to choose a water mass flow rate so that this temperature difference can be easily measured. If the water mass flow rate is too high, the gradient between inlet and outlet becomes too small and difficult to measure. For example, when this difference is 1 °C, a measurement accuracy of ±0.2 °C would translate into a 20 % uncertainty on the cooling power (neglecting the accuracy of the mass-flow meter and the estimation of distilled water properties);
- a fine control of the heating power is needed to modulate the effective cooling power provided to the internal air and keep the air temperature within a range of ±0.2 °C;

- the radiative heat exchanges between the test sample and the absorber plate will be carefully estimated, since they represent an anomalous situation compared to a typical installation in an indoor space.

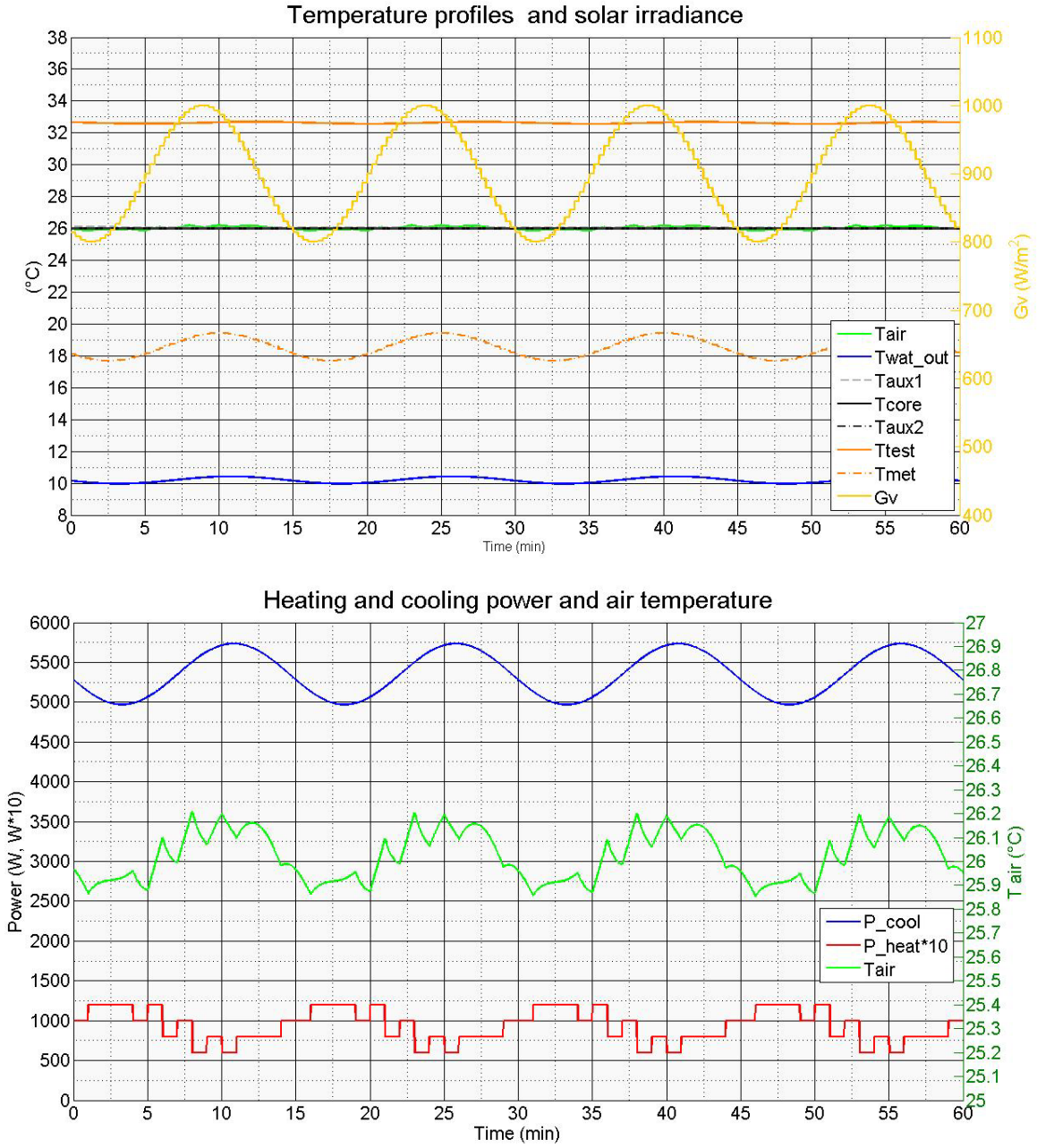

Figure 5. Simulation results - temperature profiles in the Box envelope and solar irradiance (top); heating and cooling power and air temperature inside the metering box (bottom). Note that the heating power level is multiplied by a factor 10 for ease of reading.

5. Future steps

The test cell is now under construction and will be installed and calibrated at ESTP by the early 2016. Meanwhile, various control strategies are simulated, in order to select the most promising sets of operational parameters and test them under real conditions once the test cell is installed.

Candidate technologies for the next experimental campaigns include pre-fabricated façade elements for new buildings and retrofits, integrating for example active elements (such as photovoltaic and concentration photovoltaics modules or solar thermal collectors) or decentralized mechanical ventilation systems with heat

recovery. Other likely candidates are advanced glazing systems presenting thermochromic, thermotropic or electrochromic properties and highly insulating layers such as aerogels and Vacuum Insulated Panels. The dynamic behaviour of materials such as air-permeable concrete and organic/inorganic Phase Change Materials, and the cooling properties of highly reflective coatings could also be tested under real solar radiation and wind conditions.

The output of test cell experiments will be beneficial to various target groups, such as designers and manufacturers (to boost the research and development of new products), research centres (to fully understand and model the physical phenomena occurring in a controlled space facing real outdoor conditions) and potential clients, who ask for relatively inexpensive solutions guaranteeing high levels of Indoor Environmental Quality.

6. References

[1] Marc LaFrance et al. 2013. *Technology Roadmap: Energy efficient building envelopes*, OECD/IEA

[2] Van Der Linden G.P., Van Dijk H.A.L., Lock A.J. and van der Graaf F. 1995. *COMPASS Installation guide HFS Tiles for the PASSYS Test cells*. TNO, JOULE2 Programme, Brussels.

[3] Alcamo G. *Daylight distribution and thermo-physical evaluation of new facade components through a test cell for the overheating control in Mediterranean Climate*. 5th International Conference SOLARIS, Czech Republic, 10-11 August 2011.

[4] Manz H, Loutzenhiser PG, Frank T, Strachan PA, Bundi R and Maxwell GM. *Series of experiments for empirical validation of solar gain modelling in building energy simulation codes – Experimental setup, test cell characterization, specifications and uncertainty analysis*. Building and Environment 2006, 41, 1784-1797.

[5] Van Dijk H.A.L. and van der Linden G.P. 1995. *PASLINK Calibration and component test procedures*. TNO, Delf.

[6] Van Dijk H.A.L. and Tellez F. COMPASS *Measurement and data analysis procedures*. WTCB-CSTC, Brussel, 1995.

[7] Morris Grenfell Davies, Building Heat Transfer, pagg 150-158. Wiley Ed. ISBN: 978-0-470-84731-2, 524 pages, March 2004

[8] Fraisse, G., Viardot, C., Lafabrie, O. & Achard, G., 2002. *Development of a simplified and accurate building model based on electrical analogy*. Energy and Buildings, Volume 34, pp. 1017-1031.

[9] Gouda, M. M., Danaher, S. & Underwood, C., 2002. *Building thermal model reduction using nonlinear constrained optimization*. Building and Environment, Volume 37, pp. 1255-1265.

[10] Underwood, C. P., 2014. *An improved lumped parameter method for building thermal modelling*. Energy and Building, Volume 79, pp. 191-201.

[11] Lee, K. & Braun, J. E., 2008. *Model-based demand-limiting control of building thermal mass*. Building and Environment, Volume 43, p. 1633–1646.

[12] Kramer, R., van Schijndel, J. & Schellen, H., 2013. *Inverse modeling of simplified hygrothermal building models to predict and characterize indoor climates*. Building and Environment, Volume 68, pp. 87-99.

[13] Wang, S. & Xu, X., 2006. *Parameter estimation of internal thermal mass of building dynamic models using genetic algorithm*. Energy Conversion and Management, Volume 47, p. 1927–1941.

[14] Wijeysundera, N. E., 1978. Comparison of transient heat transfer models for fiat plate collectors. Solar Energy, Vol. 2 I, pp. , Volume 21, pp. 517-521.

[15] Kamminga, W., 1985. *The approximate temperatures within a flat-plate solar collector under transient conditions*. Int. J. Heat Mass Transfer, 28(2), pp. 433-440.

[16] Schnieders, J., 1997. *Comparison of the energy yield predictions of stationary and dynamic solar collector models and the models' accuracy in the description of a vacuum tube collector*. Solar Energy, 61(3), pp. 179-190.

[17] Tagliafico, L. A., Scarpa, F. & De Rosa, M., 2014. *Dynamic thermal models and CFD analysis for flat-plate thermal solar collectors – A review*. Renewable and Sustainable Energy Reviews, Volume 30, p. 526–537.

[18] Ziegler, J.G and Nichols, N. B., 1942. *Optimum settings for automatic controllers*. Transactions of the ASME 64. pp. 759–768.

[19] Kramer, R., van Schijndel, J. & Schellen, H., 2012. *Simplified thermal and hygric building models*. Frontiers of Architectural Research, Volume 1, p. 318–325.